UNIVERSIDAD POLITECNICA DE VALENCIA

DEPARTAMENTO DE COMUNICACIONES

Máster Universitario en Tecnologías, Sistemas y Redes de Comunicaciones

Feasibility of Signaling on the Grassmann Manifold and Comparison with Coherent Techniques

Author: Akash Kadechkar

Tutor: Dr. Jose F. Monserrat

Cotutor: Dr. Daniel Calabuig

Date of start: 15/09/2015

Place: Mobile Communications Group - iTEAM

Objectives

This master thesis deals with the practical aspects of implementation of signaling based on Grassmann Manifold and its performance when compared with coherent MIMO techniques.

The objectives of this master thesis are:

- Implement the signaling approach investigated by the iTEAM.
- Test different alternatives for decoding.
- Develop the simulation framework needed for this evaluation.
- Check the feasibility in terms of computational complexity.
- Compare against other coherent techniques.

Methodology

In order to implement non coherent techniques for transmission and reception, the first step was to select the most appropriate existing theoretical developments based on the proposed techniques; in this case Grassmann Manifold was implemented. After selecting the technique and after reviewing the state of the art and expected behaviours, we broke the theoretical development into different parts to implement it separately. Before building the main simulation, it was necessary to study and execute already existing Grassmann Codes with different implementation. Then, a coherent technique was chosen for comparison with Grassmann; in this case Spatial Multiplexing. A lateral study was done on it and then a channel estimator was used for its decoding; in this case Least Square channel estimator. Then a comparison was made between Spatial Multiplexing and Grassmann using rounding off receiver, in which the received data is rounded off to its nearest possible value. Later on, the comparison was made with Maximum Likelihood Decoder for Spatial Multiplexing; in this case Sphere Decoder. The same Sphere Decoder was also used for Grassmann as we implemented Grassmann using Spatial Multiplexing. In all the encoders QAM constellations were used. Thus, at the end in all 4 transmitters and 4 receivers were implemented so as to compare their behaviour and meet the objectives of the master thesis. All the Maximum Likelihood Decoders used were actually suboptimum, as it is impossible to decode the whole block of all set of constellations together due to its computational complexity. But this suboptimum decoder is comparable to Maximum Likelihood so for practical implementation it is Maximum Likelihood Decoder.

Prototypes and laboratory work

Based on the theoretical information gathered, the implementation was done in MATLAB by simulating the coded algorithms.

Results

After implementing the hypothesis into practical simulations, respective measurements were obtained by changing parameters on signal transmission giving results for comparing the performance of Grassmann and Spatial Multiplexing.

Future research lines

In the present state of the art I could practically implement the system only in open loop. Therefore, future research lines are to implement it in closed loop. And also to compare Grassmann with many other coherent techniques other than the one used by me (i.e. Spatial Multiplexing).

Abstract

Current cellular technologies are based on the concept of coherent communication, in which the channel matrix used for demodulation is estimated via reference or pilot signals. Coherent systems involve a significant increase of signaling overhead, either when the number of Transmission Points (TP) is increased, due to the use of Coordinated Multipoint transmission/reception (CoMP) with Multiple-Input Multiple-Output (MIMO) processing, or when mobile channel changes rapidly. Another disadvantage of coherent communications is the performance degradation caused by channel estimation errors. These drawbacks of coherent communication motivate the use of non-coherent techniques. Although there are many theoretical studies on the performance of non-coherent schemes in MIMO systems, their impact on real-world cellular systems is still unknown. This thesis focuses on bringing non-coherent technique into practical system which, in this case, is Grassmann Manifold as investigated by iTEAM.

Author: Akash Kadechkar, email: akka2@teleco.upv.es

Tutor: Jose F. Monserrat, email: jomondel@iteam.upv.es

Cotutor: Daniel Calabuig, email: dacaso@iteam.upv.es

Date of defense: 20-09-16

INDEX

I. INTRODUCTION

I.1 Motivation

With more and more people using wireless communications technologies there is always a need to improve them or to design a new one. Current cellular systems use 4G communication technologies, but this technology generation will not be sufficient to meet the future and ever increasing user demands. Traffic volumes beyond the year 2020 can be even 1000 times higher than traffic volumes of today. Due to this, researchers are looking for the next generation, i.e., 5th Generation mobile networks (5G), where the European Union project Mobile Enablers for the Twenty-twenty Information Society (METIS) is playing a key role and has listed a set of requirements and scenarios to be fulfilled by 5G systems [1] and [2]. In particular, 5G systems would require higher throughput per area per user and lower latency to meet the overall targets for 5G systems: to support a large number of devices with lower energy consumption while minimizing the cost and spectrum utilization.

Current cellular technologies use coherent communication techniques, in which perfect Channel State Information is available at the Receiver (CSIR) to demodulate the received information. Training-based pilots, also known as reference signals, are used in order to estimate the CSIR, increasing the receiver complexity and the signaling overhead when the number of transmit and receive antennas increases in configurations such as Multiple-Input Multiple-Output (MIMO). Note that the receiver requires the estimation of at least $M \times N$ channel coefficients, which should be re-estimated every channel coherence interval, where M is the number of transmit antennas and N is the number of receive antennas. Coherent reception means that the coherence interval of the channel is large enough that a small portion of it can be used to send pilot symbols that will aid the receiver in the explicit estimation of the channel parameters. When this is not true, i.e., when the coherence interval is small, the receiver cannot estimate the channel parameters before they change to new, independent values. So in this case, the receiver has to proceed without explicitly estimating the channel parameters. This is called non-coherent reception, an attractive option for fast fading scenarios as coherent systems are often impractical in fast-fading scenarios as coherence time is short. Conversely, in very slowly fading channels the coherence time is of the order of a hundred times the symbol duration and the channel parameter remain constant over sufficiently many symbols for explicit estimation at the receiver, thereby enabling coherent modulation and detection methods. But with channel parameters being constant for many symbols, it tends to waste resources by sending pilots for estimating the channel for every transmission. Another disadvantage of coherent communication systems is the channel estimation errors. These systems work on the assumption that the estimated channel is perfect, but, under high mobility conditions in MIMO configuration and/or low Signal to Noise Ratio (SNR), estimated channel cannot be perfect. Thus, the above mentioned drawbacks of training based communications motivate the research on non-coherent communication techniques, which unlike coherent communication system performs data detection without any knowledge of the channel coefficients at the receiver side. This thesis focuses on bringing non-coherent technique into practical system which in this case is Grassmann Manifold as investigated by iTEAM [3].

I.2 State of Art

Growing demand for high data rates in wireless communication systems, array-based transceivers and space diversity methods have recently become an intensive area of research. Despite the absence of a-priori CSI at the receiver, non-coherent communication systems with multiple antennas can provide reliable transmission at high data rates. It has been shown, both analytically and using field tests, that in rich scattering environments, MIMO techniques can greatly increase the capacity of wireless systems [4] and [5]. Thus, state of art motivates the use of non-coherent communication techniques mostly within certain schemes with a higher number of channels to estimate such as Coordinated Multipoint transmission/reception (CoMP) or MIMO systems [6]. Preliminary research and results show that, at high SNR regimes, non-coherent communication techniques attains channel capacity of an ideal coherent system and hence performs better [7]. The transmitted signal should be designed in such a way that it can be easily demodulated at the receiver to make the non-coherent technique more feasible in a real system because, if the transmitted signal it not predesigned, then the receiver will consume more time to accurately detect the information [8].

Non-coherent techniques currently proposed in the literature can be divided into two group, types or families. One is differential encoding, and the other is independent block encoding. The first one was proposed for slow-fading scenarios based on differential transmission, in which the channel is almost constant during two signal transmission periods [9]. In this techniques, a single reference symbol, which is normally set to unity, is transmitted at first and then follows the rest of the symbols sequentially, which are all differentially encoded to their previous symbols. This family includes Differential Unitary Space-Time Modulation DUSTM [9], where transmitted signals belong to a codebook comprising a predefined set of $M \times M$ unitary matrices. The main advantage of DUSTM is its efficient decoding, which can be carried out through Multiple Symbol Differential Detection (MSSD) at the receiver side [7]. DUSTM can be seen as a higher dimensional extension of the standard DPSK modulation in accordance with the framework of non-coherent MIMO systems. The other type for non-coherent technique was proposed for block-fading channel, in which the channel coefficients are assumed to remain constant for a block of T channel uses and then changes independently to a new channel realization. On such a channel, a single code word may be transmitted after being split into several blocks, each suffering from a different attenuation, and thus realizing an elective way of achieving diversity [10]. In block fading channels capacity can be achieved with signals formed by unitary matrices multiplied by independent diagonal matrices with real nonnegative entries [11]. Later it was showed that at high SNR or when $T >> M$, capacity can be achieved with only unitary matrix signals, which motivates the use of Unitary Space-Time Modulation (USTM) [12]. USTM design was later geometrically explained as sphere packing in the Grassmann manifold [8] , which is the main motivation to use Grassmannian Constellations (GC) for block-fading channels. GC are codebooks of unitary matrices isotropically distributed on the compact Grassmann manifold. GC considers linear subspaces with orthonormal basis and MIMO channel characteristics to differentiate the transmitted symbols at the receiver side [8] and [12]. GC can be non-coherently decoded using generalized likelihood ratio test (GLRT) receivers [13] and [14]. Recent works show the utility of GC in Bit-Interleaved Coded Modulation (BICM) systems with Iterative Demodulation and Decoding (IDD) [15] and [16]. There exist many designs of GC, some of them systematic [6] [14] and [17] and others non-systematic [18]. However, so far, they have been mainly studied from a theoretical point of view. Since these constellations are gaining momentum [3] [18] [19] and [20] , this master thesis focuses on a practical implementation of GC.

I.3 Objectives

In the European project METIS (Mobile Enablers for the 2020 Information Society), the foundation of mobile and wireless communications for the fifth generation (5G) that must meet the communication needs of society from 2020 were settled. In this project, different techniques and algorithms with multiple antennas were proposed and were shown to have a great impact on the 5G. The present work takes as a starting point the results of METIS to demonstrate their viability by testing some of its deployments. This master thesis deals with the practical aspects of implementation of signaling based on Grassmann Manifold and its performance when compared with coherent MIMO techniques.

The objectives of this master thesis are:

- Implement the signaling approach investigated by the iTEAM:

  To study the investigation made by iTEAM and continue extending the investigation on the same guidelines along with practical implementation.

  While implementing Spatial Multiplexing, we found a way to implement Grassmann Manifold using Spatial Multiplexing, i.e. to implement Non-Coherent System using a Coherent System.
- Test different alternatives for decoding:

  To study the system model and finding out appropriate decoder for practical implementation.
- Develop the simulation framework needed for this evaluation:

  To develop a main simulator consisting of all the transmitters, receivers and saving the corresponding results.
- Check the feasibility in terms of computational complexity:

To make sure the system is less complex and should not take much time for the entire execution.

- Compare against other coherent techniques:
  Comparing the designed non-coherent technique with an already existing coherent technique, in this case, Grassmann Manifold (non-coherent) with Spatial Multiplexing (Coherent).

I.4 Structure of the document

The master thesis has been structured into the following chapters that are shortly outlined below:

- Chapter 2 provides a detailed study of Grassmannian Constellation (GC) and its design. It also describes Spatial Multiplexing (SM), Channel Estimation and how to transform SM into GC.
- Chapter 3 contains a simple block diagram of the entire designed simulator along with the explanation of all the scenarios and assumptions. This chapter also contains a section for the decoding principles used for detector.
- Chapter 4 includes all the results obtained under different conditions and scenarios.
- Chapter 5 summarizes the main conclusions.

II. SYSTEM MODEL

II.1 Grassmannian

Grassmannian is named after Hermann Grassmann, who introduced the concept in general. In mathematics, the Grassmannian is a space which parameterizes all linear subspaces of any finite dimensional vector space over a field **F** for given dimension $\boldsymbol{k}$. $\boldsymbol{Gr_k}\ (\mathbf{F}^{\boldsymbol{n}})$ represents the set of all $\boldsymbol{k}$-dimensional linear subspaces of $\mathbf{F}^{\boldsymbol{n}}$ where **F** is a field, $\boldsymbol{n}$ is a non-negative integer and $\mathbf{F}^{\boldsymbol{n}}$ is the standard $\boldsymbol{n}$-dimensional vector space. The Grassmannians are quite simple that their geometry is well-understood. For example, the Grassmannian $\boldsymbol{Gr_1}\ (\mathbf{F}^{\mathbf{2}})$ is the space of lines through the origin in 2-dimensional vector space as shown in figure 1(a). Similarly, $\boldsymbol{Gr_2}\ (\mathbf{F}^{\mathbf{3}})$ is the space of planes through the plane of origin in a 3-dimensional vector space as shown in the figure 1(b).

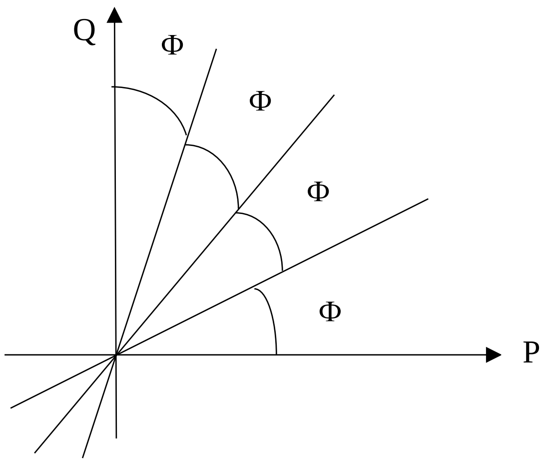

Figure 1(a): Two-dimensional vector space

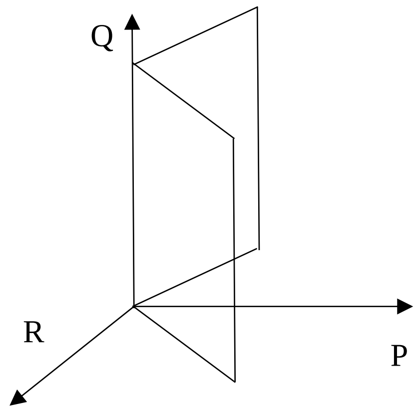

Figure 1(b): Three-dimensional vector space

The Grassmann Manifold is a space treating each linear subspace with a specific dimension in the vector space $\mathbf{F}^{\boldsymbol{n}}$ as a single point as shown in Figure 4. A subset $v_1, v_2, .., v_k$ of an $\boldsymbol{n}$ dimensional vector space with field **F**, with the inner product $< v_i, v_j >= 0$ is called orthonormal if $i \neq j$. That is to say, they are all unit vectors and orthogonal to each other. The field **F** can be real or complex number but in our case it's a set of complex numbers. An orthonormal set must be linearly independent and must have the vector space basis for the space it spans. Such a basis is called an orthonormal basis. The number of basis vectors in the field **F** is called the dimension of **F**. The simplest example of an orthonormal basis is the standard basis for Euclidean space. The vector $\boldsymbol{e_1}$ is the vector with all 0s except for a 1 in the *i* coordinate, for example: $\boldsymbol{e_1} = (1{,}0{,}0{,}0 \ldots .,0)$. A rotation or flip through the origin will send an orthonormal set to another orthonormal set. In fact, given any orthonormal basis, there is a rotation, or rotation combined with a flip, which will send the orthonormal basis to the standard basis. These are precisely the transformations which preserve the inner product, and are called orthogonal transformations. It is worth mentioning that the parameters in these decompositions give an orthonormal system .i.e. surfaces with constant parameters intersect orthogonally. It means that inside any Euclidean space, for every subspace there exist exactly only one another subspace which is orthogonal to it and linearly independent with orthonormal basis. The Grassmannian is also a homogeneous space and its subspace is determined by its basis vectors. In general, the Grassmannian can be given coordinates at a point $\boldsymbol{v_1} \in (\mathbf{F}^n)$. Let U be the open set of k-dimensional subspaces which project onto $\boldsymbol{v_1}$ and picking an orthonormal basis $b_1, \dots, b_k$ for $\mathbf{F}^n$ such that $b_1, \dots, b_k$ span $\boldsymbol{v_1}$. Using this basis, it is possible to take any k vectors and make a $k \times n$ matrix. We thus obtain the structure of a complex manifold of dimension $k \times (n-k)$. Thus, because of all the above reasons, we use Grassmannian techniques to design the constellations [12] and [8]. Several constellation design methods targeting the high SNR capacity achieving isotropic distribution have been proposed in the past [18]. Ideally, for isotropic distribution of constellations the angles between the subspaces should be equal. We have used some of those ideas to design the constellations for this Master Thesis.

As per previous studies [3], at high SNR the non-coherent capacity in block-fading channels can be achieved if the input signals are isotropically distributed unitary matrices of size $T \times M$, provided that

$$T \geq \min\{M, N\} + M \tag{1}$$

Where,

$T =$ Number of channels

$M =$ Number of transmitter antennas

These unitary matrices can be seen as M-dimensional linear subspaces lying inside a T-dimensional complex Euclidean space. The columns of the proposed signal matrices form a basis of an M-dimensional subspace. Furthermore, each matrix X is a point in the Grassmann manifold, which is the set of all M-dimensional linear subspaces of Euclidean space. Figure 1(a) shows an exemplary GC composed of five different directions in a plane, which can be represented by five 2×1 matrices, i.e. five one-dimensional subspaces in a two-dimensional space. Moreover, figure 1(b) represents two 3×2 matrices, i.e. two two-dimensional subspaces in a three-dimensional space. When the input signal matrix X is passed through the channel, the column vectors that span the original M-dimensional subspace are rotated and scaled, but they still lie within the same subspace. On the other hand, the noise does affect the subspace, but its effect can be neglected at high SNR. The particular subspace basis rotation is not detectable by a receiver without channel knowledge however, the M-dimensional linear subspace spanned by this basis can be detected by using a Maximum Likelihood Receiver with the help of channel estimator which projects the received signal on the different subspaces that compose the GC. Then, it calculates the energies of all the projections and selects the projection that maximizes the energy.

An exemplary procedure for transmission and detection of GC is described next. Figure 2 shows the block diagram of the previously associated non-coherent transceiver which uses $M = 1$ antenna, $T = 2$ time slots and the GC in Figure. Moreover, Figure 3 shows new non-coherent transceiver which has been proposed to implement in this Master Thesis.

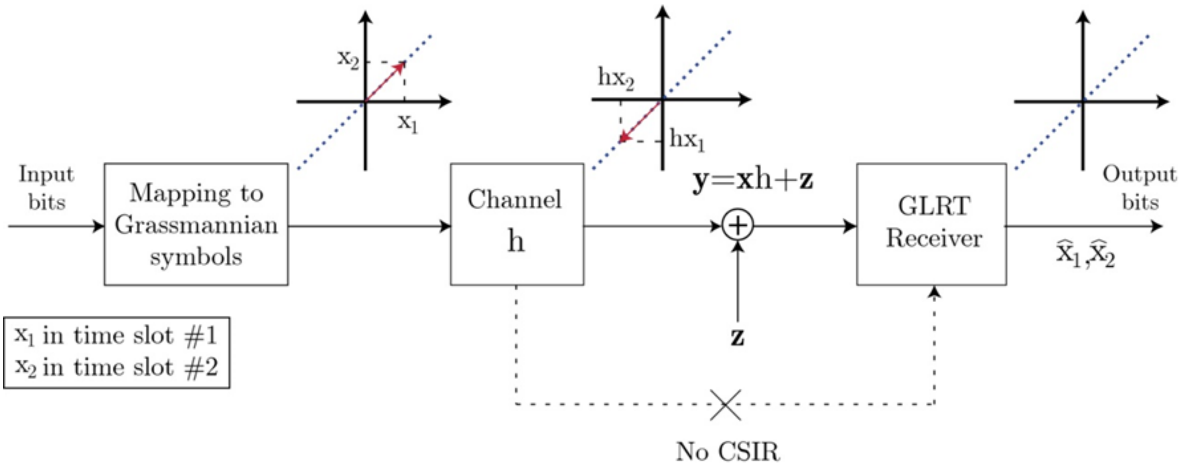

Figure 2: Existing non-coherent transceiver

As we can see in the above Figure 2, the input bits $\mathbf{x_1}$ and $\mathbf{x_2}$ are mapped to grassmannian symbols, i.e. input bits are encoded by Grassmanian Codewords or Constellations. Chordal Frobenius norm is the metric for the rate-centric design of Grassmannian constellations, that is to say, the metric to measure the distance between constellation points. And from previous experiments [18] we know that Grassmannian Codes can be designed in three different methods: Greedy Algorithm, Direct Design and Rotation-Based Design. These techniques offer different tradeoffs between the minimum distance of the constellation and the design complexity. In addition, the rotation-based technique results in constellations that have lower storage requirements and admit a natural “quasi-set-partitioning” binary labeling. In order to use Grassmannian constellations in a practical coded communication system, one typically needs to assign a binary label to each point of the constellation, so the above implemented system uses rotation-based technique with binary labeling to design constellations. The input bits are encoded by these constellations before being transmitted to the channel h. And at the receiver a GLRT (Generalized Likelihood Receiver Test) test is used to decode the received data. However, performance of this detector is comparable to that of the maximum likelihood detector, but it requires considerably less computational effort. On the other hand, the newly proposed non-coherent transceiver is slightly different as shown below in the Figure 3. Here we use the same Grassmannian Codes for modulation of the input bits and then exploit these encoded data using two orthogonal matrices with orthonormal basis such that they act like training based pilots uniformly distributed among the entire encoded data [8]. And, obviously, at the receiver, before demodulation, we used these orthogonally separated matrices to retrieve back the encoded data for the decoder to decode it.

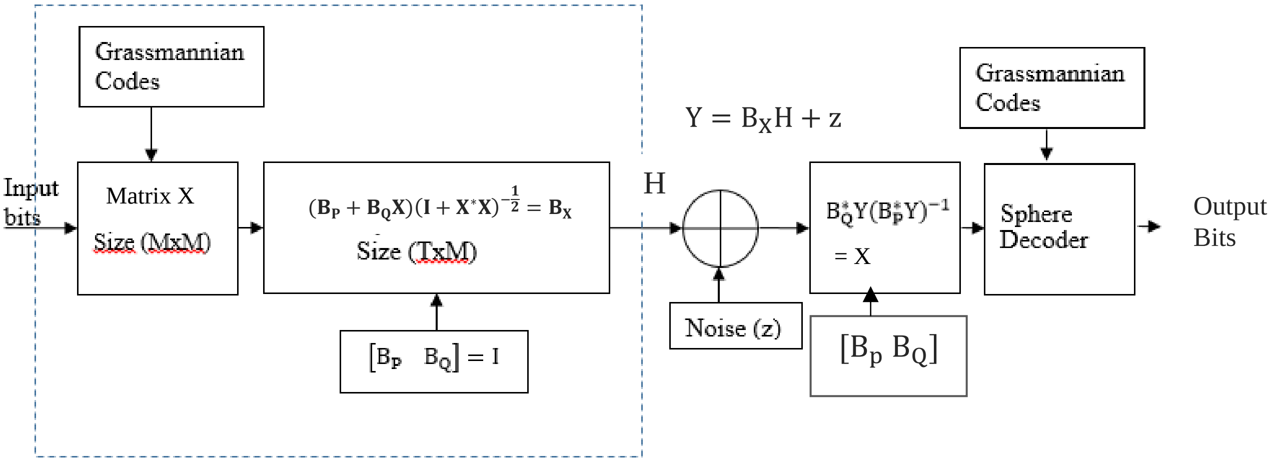

Figure 3: Proposed non-coherent transceiver

The two orthogonal matrices with orthonormal basis are nothing but an analogy to orthogonal subspaces with orthonormal basis with degree of freedom equal to 2 because we know that for every subspace there exist exactly only one another subspace which is orthogonal to it and linearly independent with orthonormal basis.

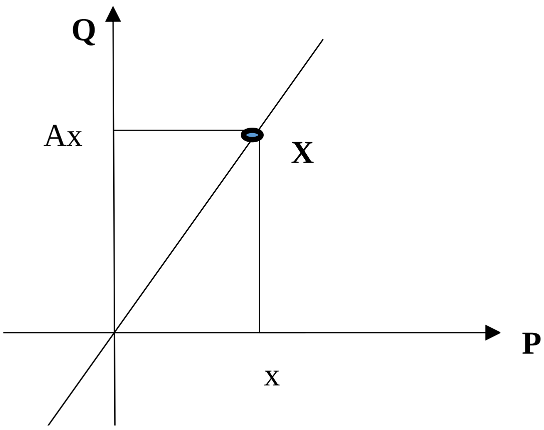

Figure 4: Two-dimensional vector space

As shown in Figure 4, using above descriptions we know that grassmannian can be given coordinates and here the coordinates of point **X** is given by equation (2).

$$\mathbf{X} = \begin{pmatrix} x \\ Ax \end{pmatrix} \tag{2}$$

$$[\mathbf{B_P} + \mathbf{B_Q}] = \mathbf{I}$$

where $\mathbf{B_P}$ and $\mathbf{B_Q}$ are two randomly generated matrices representing orthogonal subspaces **P** and **Q** respectively with orthonormal basis.

$$[\mathbf{B_P} + \mathbf{B_Q}]\begin{bmatrix} \mathrm{X} \\ \mathrm{Ax} \end{bmatrix} \tag{3}$$

X is then exploited by orthogonal subspaces **P** and **Q**.

$$[\mathbf{B_P} + \mathbf{B_Q}]\begin{bmatrix} \mathbf{I} \\ \mathbf{X} \end{bmatrix} = \mathbf{B_P} + \mathbf{B_Q X}$$

Simplifying the above equation, we get

$$(\mathbf{B_P} + \mathbf{B_Q X})^* \, (\mathbf{B_P} + \mathbf{B_Q X}) = \; (\mathbf{I} + \mathbf{X}^*\mathbf{X})^{-\frac{1}{2}}$$

$$(\mathbf{B_P} + \mathbf{B_Q X})(\mathbf{I} + \mathbf{X}^*\mathbf{X})^{-\frac{1}{2}} = \mathbf{B_X} \tag{4}$$

Equation $\mathbf{B_X}$ represents the final output of the Transmitter.

$$(\mathbf{I} + \mathbf{X}^*\mathbf{X})^{-\frac{1}{2}}(\mathbf{B_P} + \mathbf{B_Q X})^* \, (\mathbf{B_P} + \mathbf{B_Q X})(\mathbf{I} + \mathbf{X}^*\mathbf{X})^{-\frac{1}{2}} = \mathbf{I}$$

The below mentioned condition is necessary to be qualified or satisfied before sending from the transmitter because as you can see the product is an identity which means even after rotation or transformation of the basis by the channel it will remain in the same subspaces retaining all the original properties.

$$\mathbf{B_X^* B_X} = \mathbf{I} \tag{5}$$

At receiver we receive this,

$$\mathbf{Y} = \mathbf{B_X H} \tag{6}$$

where H is the channel matrix.

In order to get back the GC we do the inverse of the computation done in the transmitter and the non-coherent receiver cannot detect the particular transformation caused by the channel but can detect the subspace spanned by its basis. Hence, each of the equation (7) and (8) retrieves one half of the information and when we combine both we get back the GC as shown in equation (9).

$$\mathbf{B_Q^* Y} = \mathbf{X}(\mathbf{I} + \mathbf{X}^*\mathbf{X})^{-\frac{1}{2}} \; \mathbf{H} \tag{7}$$

$$\mathbf{B_P^* Y} = (\mathbf{I} + \mathbf{X}^*\mathbf{X})^{-\frac{1}{2}} \; \mathbf{H} \tag{8}$$

Thus, because of the properly designed transmitted matrix, the transmitted information can be recovered without any CSIR

$$\mathbf{B_Q^* Y}(\mathbf{B_P^* Y})^{-1} = \mathbf{X} \tag{9}$$

The first step for systematic design of $\mathbf{B_P}$ and $\mathbf{B_Q}$ is to construct a non-unitary complex matrix, depending on the dimension of the linear subspace which is T in our case making the size of non-unitary complex matrix $\boldsymbol{S} = T \times T$. Once the non-unitary complex matrix is constructed, its corresponding unitary matrix is obtained using the **QR** decomposition, such as $\mathbf{S} = \mathbf{QR}$. The unitary matrix used for transmission is only $\mathbf{Q}$ which is divided into two matrices $\mathbf{B_P}$ and $\mathbf{B_Q}$ with size $T \times M$ respectively. The main advantage is that they do not need to be stored at the transmitter and at receiver side and only their design rule is necessary.

II.2 Spatial Multiplexing

Spatial multiplexing (SM) is a transmission technique in MIMO wireless communication to transmit independently and separately encoded data signals from each of the multiple transmit antennas. Therefore, the space dimension is reused, or multiplexed, more than one time. In rich scattering environments, independent data signals transmitted from different antennas can be uniquely decoded to yield an increase in channel capacity which increases data rate. The number of users, or data rate of a single user, can be increased by the factor of number of transmitting antennas (M) for the same transmission power and bandwidth. Individual transmitter antenna power is scaled by $1/M$ thus the total power remains constant and independent of number of M.

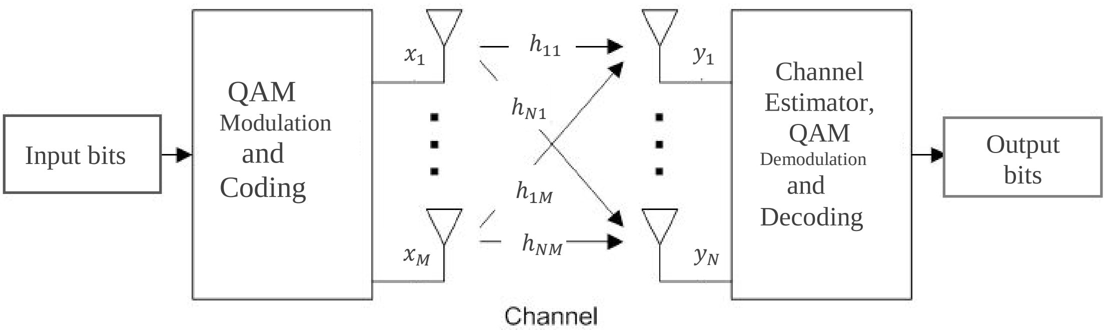

Figure 5: Two-dimensional vector space

$$\begin{bmatrix} y_1 \\ y_2 \\ \vdots \\ y_N \end{bmatrix} = \begin{bmatrix} h_{11}\ h_{12} \dots h_{1M} \\ h_{21} h_{22} \dots h_{2M} \\ \vdots \quad \vdots \quad \vdots \quad \vdots \\ h_{N1} h_{N2} \dots h_{NM} \end{bmatrix} \begin{bmatrix} x_1 \\ x_2 \\ \vdots \\ x_M \end{bmatrix} + \begin{bmatrix} n_1 \\ n_2 \\ \vdots \\ n_M \end{bmatrix}$$

If the transmitter is equipped with M antennas and the receiver has N antennas, the maximum spatial multiplexing order or the number of streams is $N_s = min\ (M, N)$. If a linear receiver is used then N_s streams can be transmitted in parallel, ideally leading to an N_s increase of the spectral efficiency, i.e. the number of bits per second and per Hz that can be transmitted over the wireless channel. The practical multiplexing gain can be limited by spatial correlation, which means that some of the parallel streams may have very weak channel gains. As shown in Figure (5) the input bits are modulated using any modulation techniques but, in this case, we chose QAM and the reason why we chose QAM is explained later in the document. More precisely, we used 4-QAM for simulations. The modulated symbols are then transmitted using transmitter antennas and in an open-loop MIMO system with M transmitter antennas and N receiver antennas, the input-output relationship can be described as

$$\boldsymbol{y} = \mathrm{H}\boldsymbol{x} + \boldsymbol{n} \tag{10}$$

where $\boldsymbol{x}$ is a $M \times 1$ vector of transmitted symbols, $\boldsymbol{y}$ is $N \times 1$ vector of received symbols with $N \times 1$ vector of noise and $\mathbf{H}$ is $M \times N$ matrix of channel coefficients. If matrix $\mathbf{H}$ is known, cross components can be calculated at the receiver. The receiver can also perform channel estimation other than the obvious QAM demodulation of received symbols. Often encountered problem in open loop spatial multiplexing is to guard against instance of high channel correlation and strong power imbalances between the multiple streams however closed-loop MIMO system utilizes Channel State Information (CSI) at the transmitter and is therefore used for communication in automobiles. In most cases, only partial CSI is available at the transmitter because of the limitations of the feedback channel.

II.3 Channel Estimator

In order to use the advantages that MIMO systems can offer, an accurate channel state information (CSI) is required at the transmitter and/or receiver. Therefore, an accurate channel estimation plays a key role in MIMO communications. One of the most popular and widely used approaches to the MIMO channel estimation is to employ pilot signals or training sequences to estimate the channel based on the received data and the knowledge of training symbols. There exists different types of channel estimators such as Least Squares (LS), Minimum Mean Square Error (MMSE), Reduced Minimum Mean Square Error (RMMSE), Scaled Least Squares (SLS), etc. which offer different tradeoffs in terms of performance, so each estimator is used depending on the system requirement [21]. And for training based on flat block fading MIMO channel estimation we chose traditional LS estimator which does not require any knowledge about the channel parameters. The task of a channel estimator is to recover the channel matrix **H** based on the knowledge of received matrix **Y** and Pilot matrix **P**.

$$\mathbf{X} = \begin{bmatrix} \mathbf{P} \\ \mathbf{D} \end{bmatrix}$$

$$\mathbf{Y} = \begin{bmatrix} \mathbf{Y_P} \\ \mathbf{Y_D} \end{bmatrix}$$

$$\mathbf{Y_P} = \mathbf{HP} + \mathrm{z} \tag{11}$$

Knowing **P** and received pilot vector $\mathbf{Y_P}$, the realization of the channel matrix can be estimated using the LS approach as follows,

$$\mathbf{H}_{LS} = \mathbf{Y_P}\mathrm{P}^{\dagger} \tag{12}$$

where $\mathrm{P}^{\dagger} = \mathbf{P^H}\left(\mathbf{PP^H}\right)^{-\mathbf{1}}$ is the pseudoinverse of **P** and $(.)^{\mathrm{H}}$ denotes the Hermitian transpose. We will use the following transmitted training power constraint:

$$\|\mathbf{P}\|_{\mathrm{F}}^{2} = \mathcal{P} \tag{13}$$

where $\mathcal{P}$ is a given constant value and ||•|| is the Frobenius matrix norm.

Hence, pilot is calculated as

$$\mathbf{P} = \sqrt{\frac{\mathcal{P}}{Nt}}\begin{bmatrix} 1 & 1 & \cdots & 1 \\ 1 & W_N & \cdots & W_N^{N-1} \\ \vdots & \vdots & & \vdots \\ 1 & W_N^{t-1} & \cdots & W_N^{(t-1)(N-1)} \end{bmatrix} \tag{14}$$

where $W_N = e^{j2\pi/N}$ and $N \geq t$

N = number of pilots

t = number of transmit antennas

In our case, $N = t$.

Now from the pilots **P** and received vector $\boldsymbol{y}$ we can estimate the channel $\mathbf{H}_{LS}$ as shown in equation (12). Using $\mathbf{H}_{LS}$ the information vector A can be retrieved back by multiplying the received data vector $\mathbf{Y_D}$ with the inverse of estimated channel.

$$\mathbf{X} = \mathbf{Y_D} * \mathrm{inv}(\mathbf{H}_{\mathrm{LS}}) \tag{15}$$

II.4 SM to GM

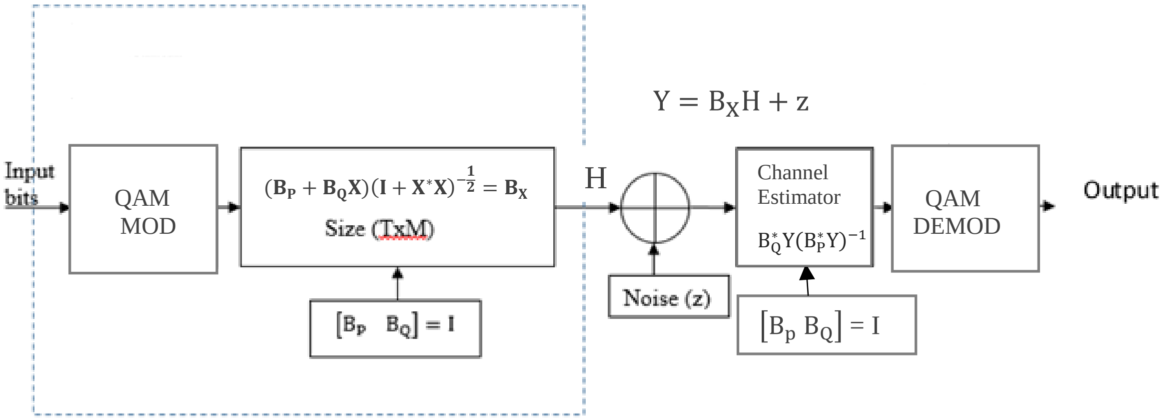

Figure 6: SM to GM non-coherent transceiver

As from the above explanations, we know that in SM the transmitted block consists of pilot symbols at the start and then follows the actual data symbols which are encoded by 4-QAM constellation. And in GM, unlike SM the pilot symbols are uniformly distributed along the entire transmitted block.

Comparing equation (9) and (15)

$$\mathbf{B_Q^* Y (B_P^* Y)^{-1}} = \mathbf{Y_D} * \mathrm{inv}(\mathbf{H}_{\mathrm{LS}}) \quad (16)$$

Hence we can conclude that,

$$\mathbf{B_Q^* Y} = \mathbf{Y_D} \quad (17)$$

$$\mathbf{B_P^* Y} = \mathbf{H_{LS}} \quad (18)$$

Thus, from equation (17) and (18), we can say that $\mathbf{B_Q^* Y}$ is the received information vector $\boldsymbol{Y}_\mathbf{D}$ and $\mathbf{B_P^* Y}$ is the estimated channel $\mathbf{H}_{\mathrm{LS}}$.

So, we can design a Grassmannain (GM) transceiver system using a Spatial Multiplexing (SM) transceiver system. Even better, we can say that we can design a non-coherent communication system using a coherent communication system using the above guidelines. To design uniformly distributed Grassmannian Constellations for higher dimensions it is very complex, hence we tend to design constellations similar to QAM constellations with two degrees of freedom. Now, as we know, we can design GM from SM. Therefore, we can use QAM constellations itself for modulation instead of Grassmannian Codes, which is a code book of bigger size and is needed to be stored or at least computed at the transmitter as well as receiver, whereas QAM is smaller size and can be easily computed at the transmitter as well as receiver using design rule. Hence, Figure (6) is the block diagram of SM with additional computational block at the transmitter making it a GM non-coherent transceiver. Hence, with proper designing of the data at the transmitter it is possible to retrieve the modulated data using LS channel estimator at the receiver. Although it is also a GM non-coherent system, it is not better than the GM non-coherent system with Grassmannian Codes as the QAM constellations are not as compact and, most importantly, it is not exactly uniformly distributed. However, this system has been implemented in this master thesis as it is less complex, less time and resource consuming and, moreover, it has not been implemented before.

III. METHODOLOGY

III.1 Simulation

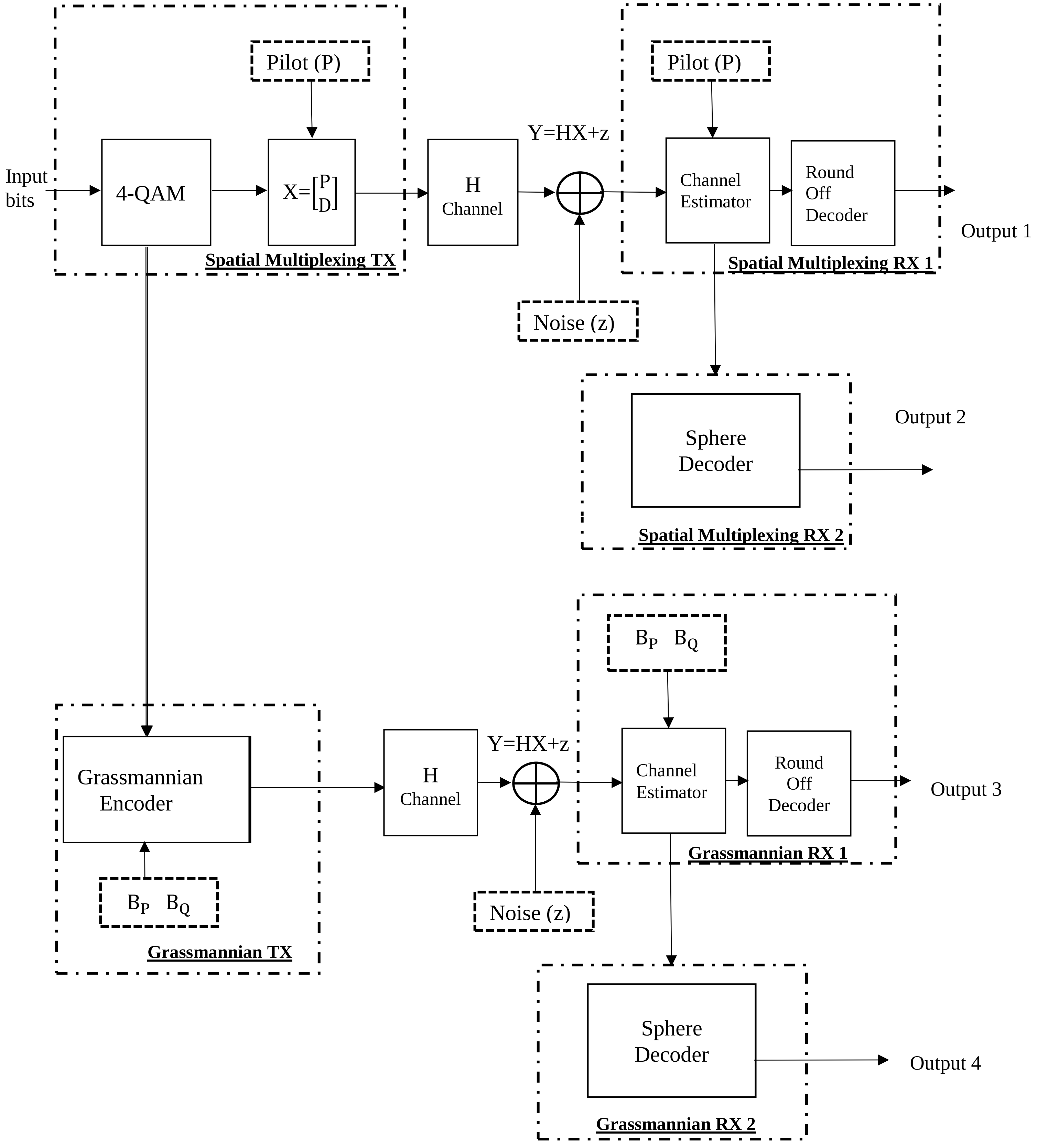

Figure 7: Overall block diagram of the simulator

We consider a block-fading channel that remains constant during T time slots to evaluate the joint coherent and non-coherent communication. Depending on the configuration of transmitter and receiver antennas, we have two main types of scenarios. In the first scenario there is 2 TPs with a single antenna each, i.e. $M = 2$ transmitter antennas, to a single user with $N = 2$ antennas and T is varied from 4 to 16 and for the second scenario M depends on the T such that $M = T/2$, where T is varied from 2 to 10. The bits per channel use (*bpcu*) determines the transmission rate of the system and is calculated using all the variables used in the transmission such as T and M. To prove the interest of non-coherent communication based on GC, this scheme is to be compared with codes designed for the same total number of antennas, input bits and average transmit power that need to be coherently decoded (with CSIR). To be consistent with previous works, we selected a coherent (training-based) baseline. In particular, for 2 transmitter antennas the transmitter output is a matrix of size $T \times M$ where $M = 2$ and $T \geq 2 \cdot M$. The GC scheme is compared to open-loop coherent scheme called SM designed for the same total number of antennas. The coherent baselines are based on the training bits or pilot symbols as defined in equation (14) and [21]. Pilot symbols are based on the M time slots for training the coherent schemes. 4-QAM modulation scheme was chosen to encode bits into symbols. As we used SM to generate GC, we did not use GC codebook of size 256, 2048 or 4096 bits as used in earlier version as shown in Figure 2. Because of the use of QAM for generating symbols, it was easy to vary the values of many parameters such as T,M, *bpcu*, etc. which is much complex in case of GC codebook of fixed size. We can achieve a transmission rate of upto 8 *bpcu*. For example, if $T = 4$ and *bpcu*=8, then 32 bits are transmitted in 4 time slots.

We use two transmitters, one for SM with the training based pilot symbols at the beginning of each block so that it can be easily decoded at the receivers. The other transmitter is based on the concept of Grassmann derived from SM. In general, for GM we distribute the pilots uniformly among all the symbols, for that we consider a unitary matrix which we separate it into two matrices such that they are orthogonal to each other with orthonormal basis of their respective subspaces. We call them $\mathrm{B_P}$ and $\mathrm{B_Q}$ as shown in the Figure 7. The 4-QAM symbols are then computed with $\mathrm{B_P}$ and $\mathrm{B_Q}$ as shown in equation (7) and (8) to get the desired transmit matrix $\mathrm{B_X}$ of size $T \times M$ as shown in equation (9). The first condition which is needed to be passed in order to proceed the simulation further is the average power of the transmit matrix which should be constant or equal for all the transmitters. However, it is to be noted that the average power here depends on the number of transmitter antennas. For the first scenario $T > M$, the number of transmitter antenna $M = 2$. Hence, I scaled the average transmit power of SM to 2. As we know GM are assumed to be uniformly distributed constellations and its column vectors which in this case is M determine the average power. However, for SM the M determines the average power of only the pilots and with the information bits the average power is more than M, so we need to scale down the average power of SM equal to M. In case of second scenario $T = 2M$, average power for different M ranging from 2 to 5 was equal for both the transmitters after scaling down SM transmit matrix. If the average power in both the transmitters is not equal to M, then the results we get are not comparable. Because a transmitter with more average power will have a better chance of getting detected at the receiver than the transmitter with less average power. Thus, for comparisons to be fair it is necessary to test both the transmitters under similar conditions under same average power. SM scheme uses two receivers, one receiver has a round off decoder which rounds the received data to its nearest constellation value and it's easy to implement, and, the another receiver is Sphere Decoder which decodes the received data based on the probability of most likely event. It is also referred to as a Maximum Likelihood Decoder for SM in practical conditions and in the later section it has been explained in detail. GM also uses the same two receivers. By assuming that the communication system operates in the low-to-high SNR region, one can gain insight in the manner in which the coherence time T affects the achievable data rate.

III.2 Decoding principles

Decoding the received signal is the most important critical part of the system. The decoder determines the correctness, efficiency and feasibility of any communication system. The decoder should be as less complex and less time consuming as possible but of all the most important use of the decoder is to retrieve the correct information from the received signal. There are in theory many types of decoders starting from round off decoder till the maximum likelihood decoder. Round off decoder is the simplest and the least complex decoder. In round off decoder the constellations received from the received signal are rounded off to the nearest or the closest value from the set of reference constellations. However, it does not give very good results in practical applications under high SNR. There are other decoders that give better results than round off at high SNR but such decoders are quite complex and also consume a lot of time for execution. One of such decoders is the Maximum Likelihood decoder, which chooses constellation with maximum probability out of the list rather that the nearest value.

In this Master Thesis, we have used both round off decoder as well as maximum likelihood decoder in the receivers of both Spatial Multiplexing and Grassmann Manifold. However, the maximum likelihood decoder is in fact a Schnorr-Euchner Sphere Decoder (SESD), which is suboptimum and is not actually a maximum likelihood decoder in theory. We do not use a maximum likelihood decoder because it is not feasible and is impossible to implement a maximum likelihood decoder in practise. As per the definition of maximum likelihood decoder, it will select a value with highest probability out of the entire set. But in real life scenario the entire constellation set is very large as we transmit different number of constellations like in number of millions and the receiver should receive the transmitted constellations as soon as possible, otherwise the information will be lost in the channel. Moreover, it is not possible for the receiver to store all the received information from the transmitter and decode it at once, as the transmitted constellations will be in millions and receiver will not have that much memory space and, more importantly, it will take years of time to collect and decode it at once. And if the transmitted message is not received and decoded on time, it cannot be used for practical or real life scenarios. So, in practice, we do not transmit the entire huge block of data but we transmit a number of small sized blocks so that receiver can receive and decode it at that instant so that the purpose of communication is meaningful. In addition, if we cannot have the entire constellation set for decoding, then the decoder can't be a maximum likelihood decoder. So, in theory SESD is not a maximum likelihood decoder, but in real life scenario we can consider it as comparable to Maximum Likelihood Decoder (MLD).

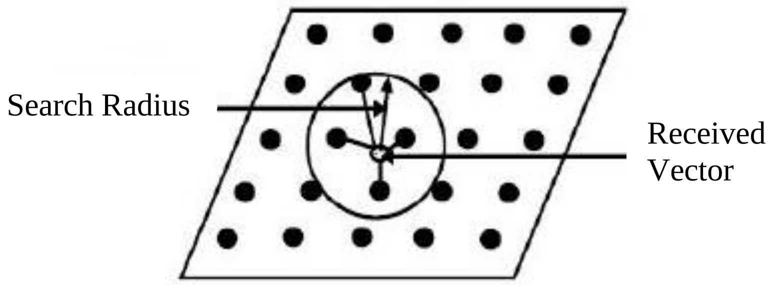

Figure 8: Sphere decoder

SESD intends to find the transmitted constellation vector with minimum ML metric, i.e. to find ML solution vector. Unlike MLD, it considers only a small set of constellation vectors within a given sphere rather than all possible transmitted constellation vectors. However, SESD has a drawback that its complexity depends on SNR as the SNR increases so as the computation and complexity. In SESD the received constellation vectors will be assumed as a nodes and each node will have a sphere surrounding it making the node itself as the centre of the sphere with a specific radius as shown in the above Figure 8 [22]. And the range of each node limits within its corresponding sphere. Now, all nodes will check probabilities of all the constellation vectors within their respective spheres to select that constellation vector with maximum probability of occurrence and hence decoding. But, in this process, proper care must be taken while selecting the radius of the sphere as it will always impact the detector. For example:

- If the radius is too small, then there will be very less constellation vectors or even no constellation vectors inside the search area in the sphere resulting in failure of the detector.
- And if the radius chosen is too large, then there will be too many unnecessary constellation vectors to be searched while increasing the complexity with decrease in efficiency.

IV. RESULT AND DISCUSSION

For evaluation, four schemes are compared, which are the following:

- SMR (Spatial Multiplexing with round off decoder)
- SMS (Spatial Multiplexing with SESD)
- GCR (Grassmann Codes with round off decoder)
- GCS (Grassmann Codes with SESD)

All the four schemes are made to compare with each other. But, because of the huge difference in efficiency of round off decoder and suboptimum decoder (SESD), we obviously compare SMR with GCR and SMS with GCS. All the systems use the same input bits so that an exact comparison can be made between them. Moreover, the transmitting power of both the transmitters are scaled to be equal for comparative analysis. The evaluated metric is the Block Error Rate (BLER), being T the number of channels, M the number of transmitting antenna, N is number of receiving antenna, *bpcu* is bits per channel use and SNR refers to Signal to Noise Ratio in dB.

We will first analyse the performance for a small size system, and then increase the number of antennas to check the impact on the different case scenarios/configurations as shown in the below Table 1. Later we analyse the performance of all the system configurations at a specific SNR and Table 2 represents the case scenarios for the same.

Scenario	*T*	*M=N*	*bpcu*
1	4	2	2
2	8	2	2
3	8	4	2
4	10	5	2

Table 1: Scenarios tested against varying SNR from 0 to 50 dB

Scenario	SNR (dB)	*M=N*	*bpcu*
1	20	2	2
2	18	*T*/2	*bpcu=2*M*(T-M)/T* (refer Table 3)

Table 2: Scenarios tested against varying T

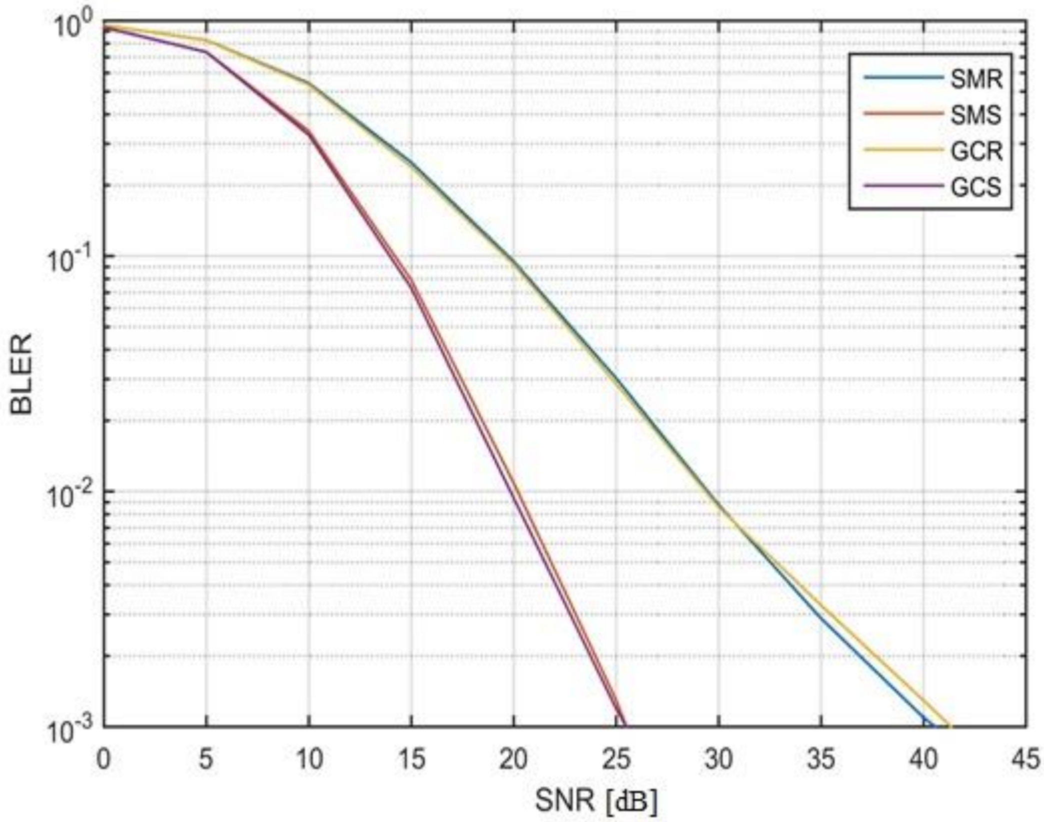

Figure 10: Performance comparison between signaling of GM and SM using round off and SESD detection when $T = 4$, $M = 2$ and *bpcu*=2.

The above Figure 10 represents BLER for the first scenario from the Table 1 where $T = 4$, $M = N = 2$ and *bpcu* = 2. The entire system is simulated under variable SNR from 0 to 50 dB. As we can see in the figure, with the same input bits there is a difference in the curve. The GCS performs better than SMS throughout the curve whereas GCR performs better than SMR until around 31 dB of SNR but after that SMR performs better. For the above mentioned scenario we can conclude that GCS performs better than the SMS in low as well as moderate SNR but GCR performs better than SMR only at low SNR. Even though there is no huge different but GCS is still better.

The below Figure 11 represents the performance comparison between signaling of GM and SM using round off and SESD detection for the second scenario from Table 1 where $T = 8$, $M = 2$ and *bpcu*$= 2$. Here, also similarly to above scenario, GCS performs better than SMS throughout the curve but the good thing here is that the GCR also performs better than the SMR. In all GM performs better than SM in low as well as moderate SNR in both the decoders for this scenario. But overall the BLER is increased for all the systems as compared to Figure 10. **As *T* increases the probability of error increases and even if there is one error the whole block is counted as error making the BLER high as *T* increases.** We can observe in Figure 11 that the curves cut BLER 10^{-3} at approx. 2-3 dB more than in the above scenario as shown in Figure 10. However, we can also notice that the increase in BLER is more in case of SMS and SMR as compared to GCS and GCR respectively. **We can**

conclude that when increasing T the performance of non-coherent schemes augment and this is aligned with the study presented in [3].

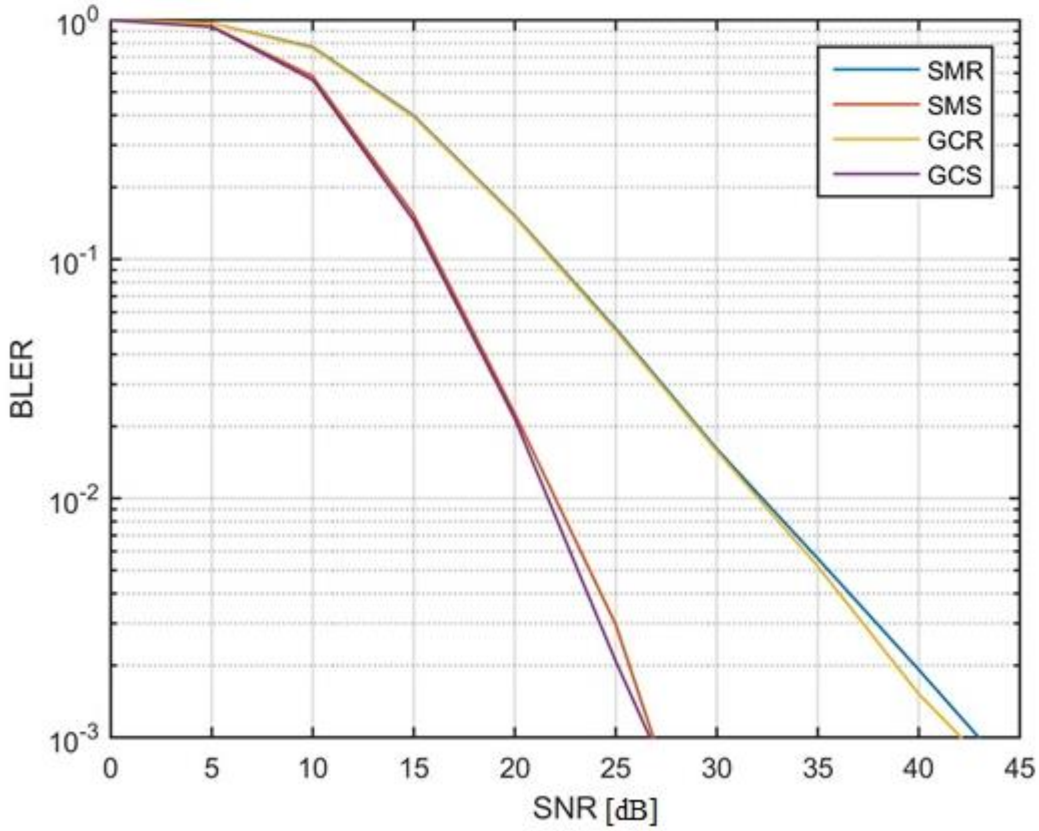

Figure 11: Performance comparison between signaling of GM and SM using round off and SESD detection when $T = 8$, $M = 2$ and *bpcu*=2.

For the below Figures 12 and 13, the condition is $T = 2M$ as shown in third and fourth scenario of Table 1 where $M = 4$ in third scenario and $M = 5$ for the fourth scenario respectively with *bpcu* $= 2$ in both cases. As we can see in Figure 12, GCS again performs better than SMS but GCR does not perform better than SMR. However, we can notice that BLER is reduced by a factor of 6-7 dB for both GCS and SMS, but increased by a factor of 1 dB for GCR as compared with Figure 11.

Similarly, Figure 13 shows that GCS performs better than SMS throughout the system and also GCR performs better than SMR after SNR 47 dB. Comparing Figure 12 and 13, we can observe that the BLER yields gain of some SNR for GM schemes as the T increases unlike the scenario where $T > 2M$. **It is because these two system configurations use $T = 2M$ with which we increase the number of antennas i.e. $M = T/2$ and this increases the capacity of the system. Hence, obviously as the M increases we achieve better BLER at less SNR as compared to when $M < T/2$. From the above comparison we can conclude that when $T = 2M$ the system gives better BLER than $T > 2M$.**

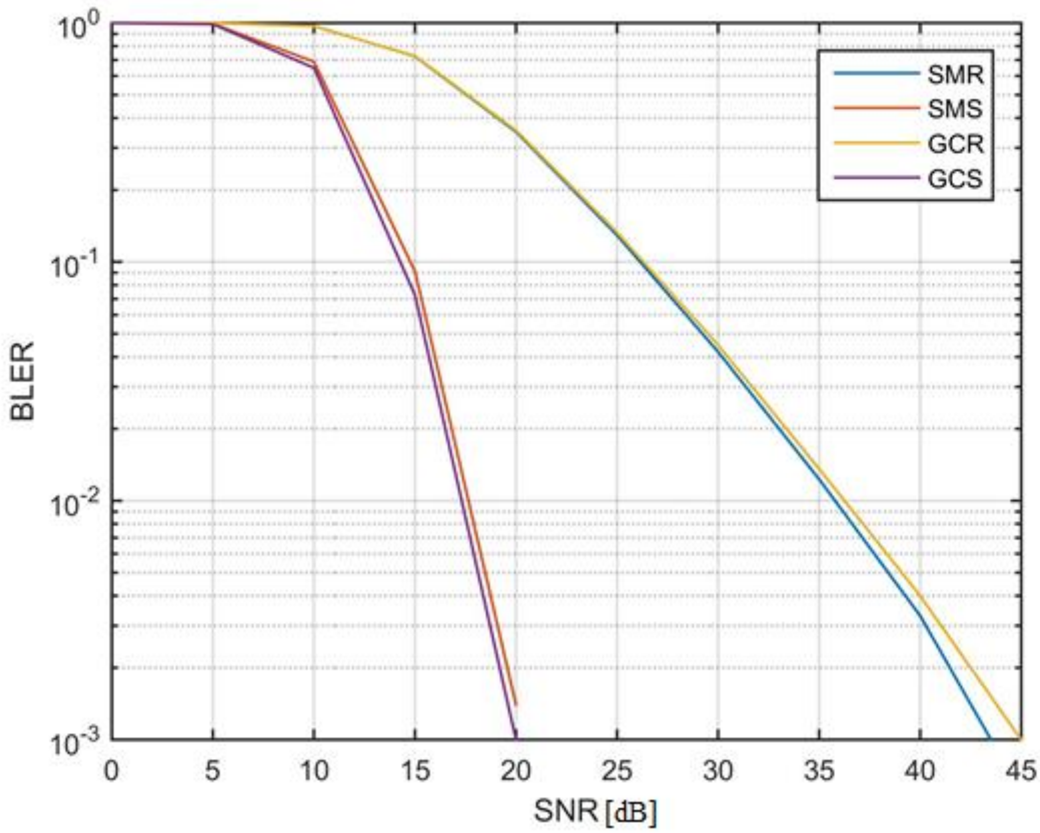

Figure 12: Performance comparison between signaling of GM and SM using round off and SESD detection when $T = 8$, $M = 4$ and *bpcu*=2.

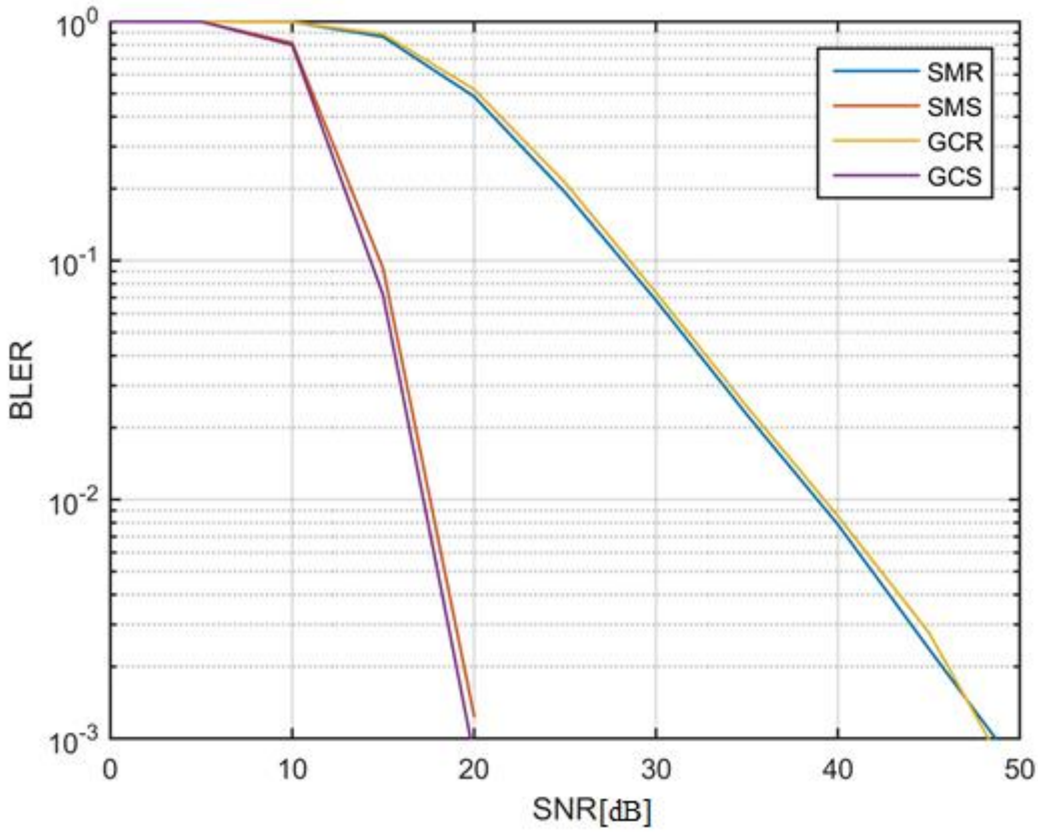

Figure 13: Performance comparison between signaling of GM and SM using round off and SESD detection when $T = 10$, $M = 5$ and *bpcu*=2.

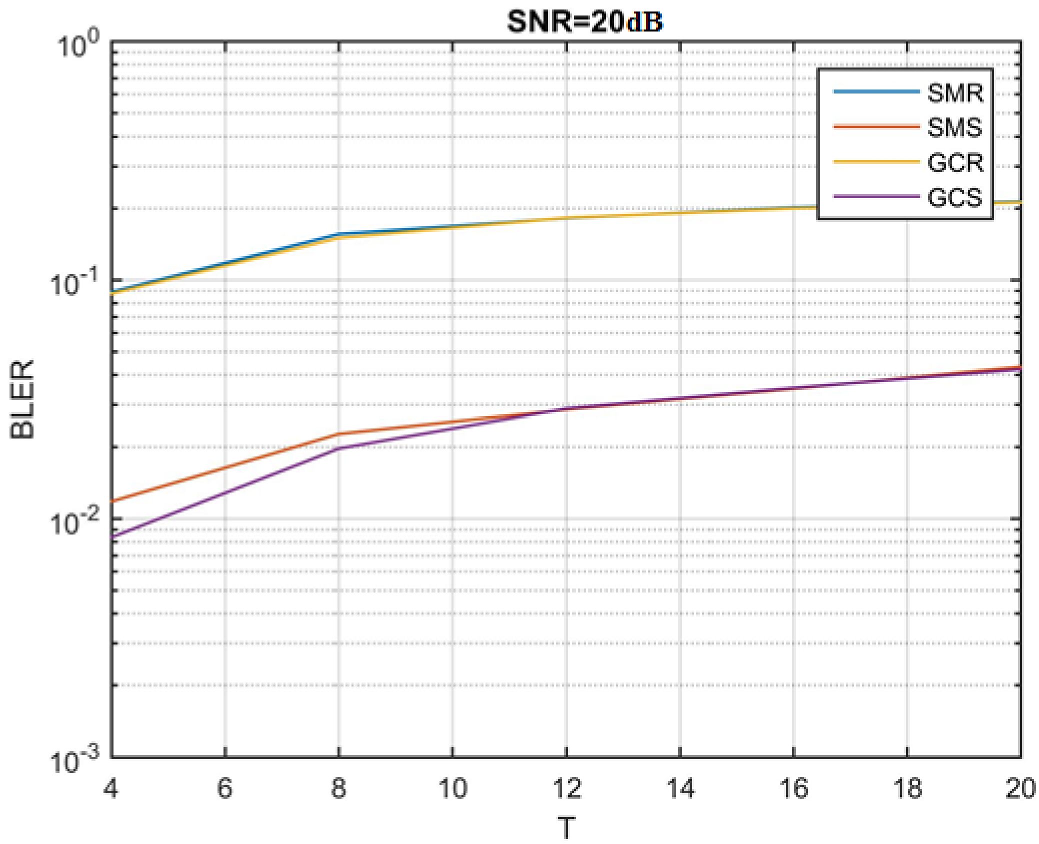

Figure 14: BLER performance of GM and SM at 20 dB of SNR with increasing T and $M = 2$

Now, testing the first scenario from Table 2 we get Figure 14, which shows the behaviour of all size systems i.e. varying T at a specific SNR which in this case is 20 and also at a specific $M = 2$, i.e. $T > 2M$. As we can see in Figure 14, SMR and GCR have almost the same throughout curve. Moreover, GCS is better than the rest of the systems at less T but as the T increases the difference is getting reduced. **As M = 2 is fixed and T is increased, the symbols used for pilots is fixed. So more information is sent and pilots are negligible in comparison to data. Hence, the difference between coherent and non-coherent curves reduces with increasing T, as expected from previous analysis [3].**

However, when we also vary M along with T as per the second scenario of Table 2, i.e. $T = 2M$ at a specific SNR=18, we observe a different curve in Figure 15, which is exactly opposite to the one in Figure 14 for the schemes using SESD. For the results in Figure 15, we fixed the modulation to 4QAM for simplicity reasons. As a result, as M increases, the bits per channel use also increases, as shown in Table 3. As we observe in Figure 15, the schemes using round off detector does not show any change as compared to Figure 14 but GCS and SMS yields better BLER as the T increases and also we can notice that as the T increases the difference between the GCS and SMS curve increases until $T = 6$ and then the difference is constant with GCS performing better. **Hence, the**

Grassmannian scheme with suboptimum ML detector (SESD) behaves better and exactly as per desired [3].

T	*M*	*bpcu*
2	1	1
4	2	2
6	3	3
8	4	4
10	5	5

Table 3: bpcu corresponding to varying M and T

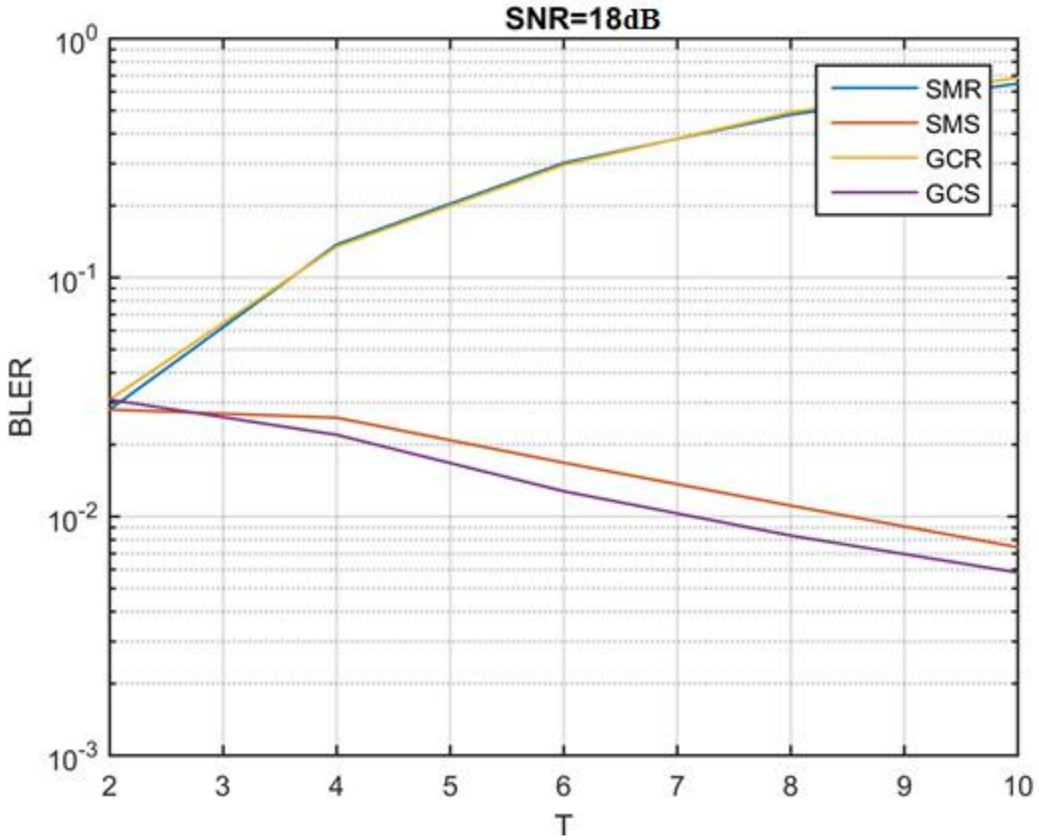

Figure 15: BLER performance of GM and SM at 18 dB of SNR with increasing $T = 2M$

V. Conclusion and future work

In this master thesis the concept of non-coherent MIMO communication was presented. Based on the research lines of iTEAM, GM scheme was the chosen non-coherent technique for MIMO communication together with some of the main techniques that enable this type of communication. As per the object of the thesis, a comparison was made between coherent and non-coherent signaling schemes under practical channel conditions. SM was selected as the coherent technique to be compared with GM. Extending the investigation on the guidelines of iTEAM, GM was implemented in a way different than the conventional method. GM was implemented using the same coherent SM scheme with which it is being compared. The performance of GM and SM schemes was evaluated in a spatially correlated block-fading MIMO system. Both GM and SM used same two detectors, i.e. round off and SESD at their respective receivers to have a comparative analysis. Despite the fact that spatial correlation is detrimental for coherent and non-coherent systems, the latter outperformed the coherent one in all the scenarios with *bpcu*=2 for SESD detector and also with round off detector non-coherent system performed better when was T increased. Furthermore, we observed that when, T increases, BLER reduces and the system performs better than SM at both low and moderate values of SNR. As the correlation between the receive antennas increases, the performance gap between both GM and SM using round off detector is reduced for $T > 2M$ as well as for $T = 2M$. But, the gap increases in favor of GM using SESD showing GM performs better than SM when $T = 2M$. From Figure 14 and 15 we can conclude that as T grows, the capacity of the non-coherent channel approaches that of the coherent one and in fact it also outperforms coherent one; from which one can conclude that if T is sufficiently long, the amount of time needed for the receiver to acquire a sufficiently accurate channel model becomes insignificant in comparison with the overall signaling interval.

Further work includes implementing the same system in closed loop applicable for vehicular communication. Investigating constellation designs for higher dimensions using the Grassmannian Constellations that mimic isotropic distribution by expanding its subspace and along with it a corresponding suboptimum non coherent ML detector. In addition, the design of MU-MIMO techniques for non-coherent coordinated communication will be also included in our way forward. Another relevant aspect to be investigated in future work is how GC could be fitted within an OFDM system. And also to compare Grassmann with many other coherent techniques other than the one used by me (i.e. Spatial Multiplexing).

Acknowledgments

This thesis is related to the research carried out by iTEAM in the framework project of METIS-II, which is partly funded by the European Union.

References

[1] B. Timus and M. Fallgren (Editors), "D1.1 Scenarios, requirements and KPIs for 5G mobile and wireless system", ICT-317669-METIS, Project Deliverable, April 2013.

[2] J. F. Monserrat and M. Fallgren (Editors), "D6.1 Simulation Guidelines", ICT-317669-METIS, Project Deliverable, October 2013.

[3] S. Roger, J. Cabrejas, D. Calabuig, J. F. Monserrat, Y. Fouad, R. H. Gohary, H. Yanikomeroglu, "Non-coherent MIMO Communication for the 5th Generation Mobile: Overview and Practical Aspects", Waves, no. 6, pp 5-13, 2014.

[4] G. J. Foschini and M. J. Gans, "On limits of wireless communications in a fading environment when using multiple antennas", Wireless Personal Communications, vol. 6, pp. 311–335, Mar. 1998.

[5] E. Telatar, "Capacity of multi-antenna Gaussian channels", Bell System Tech. J., June 1995.

[6] I. Kammoun and J. -C. Belfiore, "A new family of Grassmann spacetime codes for noncoherent MIMO systems", IEEE Commun. Lett. vol. 7, no. 11, pp. 528-530, Nov. 2003.

[7] T. Cui and C. Tellambura, "Bound-intersection detection for multiple-symbol differential unitary space time modulation", IEEE Trans. Commun., vol. 53, no.12, pp. 2114–2123, Dec. 2005.

[8] L. Zheng, D.N.C Tse, "Communication on the Grassmann Manifold: A Geometric Approach to the Noncoherent Multiple-Antenna Channel", IEEE Transactions on Information Theory, vol. 48, pp. 359-383, 2002.

[9] B. M. Hochwald and W. Sweldens, "Differential Unitary Space-Time Modulation", IEEE Trans. on Communications, vol. 48, no. 12, pp. 2041–2052, December 2000.

[10] Ezio Biglieri, Giuseppe Caire, Giorgio Taricco, "Coding for the Fading Channel: a Survey", in Byrnes, J.S. Signal Processing for Multimedia. IOS Press. p. 253. ISBN 978-90-5199-460-5, 1999.

[11] T.L. Marzetta, B. Hochwald, "Capacity of a Mobile Multiple-Antenna Communication Link in Rayleigh-Flat Fading", IEEE Transactions on Information Theory, vol. 45, pp. 139-157, 1999.

[12] B. M. Hochwald, T.L. Marzetta, "Unitary Space-Time Modulation for Multiple-Antenna Communications in Rayleigh Flat Fading", IEEE Transactions on Information Theory, vol. 46, no. 543-564, 2000.

[13] M. Beko, J. Xavier, V.A.N. Barroso, "Non-coherent Communication in Multiple-Antenna Systems: Receiver Design and Codebook Construction", IEEE Trans. on Signal Processing, vol. 55, no.12, pp. 5703-5715, Dec. 2007.

[14] I. Kammoun, A. M. Cipriano, and J.-C. Belfiore, “Non-coherent codes over the Grassmannian”, IEEE Trans. Wireless Commun., vol. 6, pp. 3657–3667, Oct. 2007.

[15] M. A. El-Azizy, R. H. Gohary and T. N. Davidson, “A BICM-IDD Scheme for Non-Coherent MIMO Communication”, IEEE Trans. on Wireless Communications, vol. 8, no. 2, pp. 541-546, February 2009.

[16] R. H. Gohary and T. J. Willink, “On LLR Clipping in BICM-IDD Non-Coherent MIMO Communications”, IEEE Communications Letters, vol. 15, no. 6, pp.650-652, June 2011.

[17] J.-K. Zhang, F. Huang, S. Ma, “Full Diversity Blind Space-Time Block Codes”, IEEE Trans. on Information Theory, vol. 57, no. 9, pp. 6109-6133, September 2011.

[18] Ramy H. Gohary, Timothy N. Davidson, “Noncoherent MIMO Communication: Grassmannian Constellations and Efficient Detection”, IEEE Transactions on Information Theory, vol. 55, no. 3, March 2009.

[19] S. Roger, D. Calabuig, J. Cabrejas, J.F. Monserrat, “Multi-user non-coherent detection for downlink MIMO communication”, IEEE Signal Process Letters, vol. 21, no. 10, pp. 1225–1229, 2014.

[20] Y. M. M. Fouad, R. H. Gohary, J. Cabrejas, H. Yanikomeroglu, D. Calabuig, S. Roger, J. F. Monserrat, “Time-Frequency Grassmannian Signalling for MIMO Multi-Channel-Frequency-Flat Systems”, IEEE Communications Letters, vol. 19, no. 3, pp. 475-478, March 2015.

[21] Mehrzad Biguesh, Alex B. Gershman, “Training-Based MIMO Channel Estimation: A Study of Estimator Tradeoffs and Optimal Training Signals”, IEEE Transactions on Signal Processing, vol. 54, no. 3, March 2006.

[22] R. P. Yadav, Garima Mathur, Sonjuhi Mrinalee and Honey Priya Garg, “Improved radius selection in sphere decoder for MIMO System”, International Conference on Computing for Sustainable Global Development (INDIACom), 2014